Proc Indian Natn Sci Acad **80** No. 3 September 2014 pp. 633-645
É *Printed in India*.
10.16943/ptinsa/2014/v80i3/55139

Research Paper

Hand Tremor Quantification Using Virtual Object Manipulation in a Haptic Environment

K SAJITH*, PREETI GOPAL and SUBHASIS CHAUDHURI
Department of Electrical Engineering, Indian Institute of Technology Bombay, Powai, Mumbai, India

(Received on 17 September 2013;Revised on 05 March 2014;Accepted on 10 May 2014)

We have developed a virtual haptic system for detection and quantification of hand tremor by manipulating an object in a virtual environment. The subject performs the task of moving a soft object from one point to another in a virtual 3D environment using a haptic device. The velocity of hand motion is collected by a haptic device while the task is being performed. The collected velocity data is processed to extract the tremor, if any. The extracted tremor data is subjected to spectral estimation using auto-regressive (AR) modeling to determine the tremor frequency and the Choi-Williams spectral estimation is performed to observe the variability of tremor frequency with time. The proposed method is validated by simultaneously capturing motion sensor data and comparing the performances.

Key Words: Accelerometer; Deformable Object Rendering; Hand Tremor; Haptics; Spectral Estimation

Introduction

Tremor is an involuntary oscillatory movement of body parts. Tremor is one of the most important symptoms of different types of neurological disorders. Tremor can affect various body parts such as hands, head, facial structures, tongue, trunk and legs. Most tremors occur in the hands. Tremor often accompanies neurological disorders associated with aging. Although tremor by itself is not a life threatening disorder, it can cause functional disability and social embarrassment to the aged. Physical disabilities regarding pathological hand tremor may make it difficult or impossible for individuals to perform several simple jobs like picking a pen from a table, moving a light weight object, opening a door, etc. According to the behavioural context or position, tremor is classified as resting, postural, kinetic and task specific. The most incapacitating tremors are essential tremor, tremor due to Parkinsonõs disease and cerebellar tremor. Resting or static tremor occurs when the muscle is at rest. This type of tremor is mostly associated with Parkinsonõs disease. Postural tremor occurs when a patient attempts to maintain a posture. Kinetic tremor occurs during a purposeful movement. Task specific tremor appears while performing goal oriented tasks such as handwriting (Rocon *et al*., 2004). Detection, quantification and rehabilitation of hand tremor have a great impact on the affected people. Commonly used techniques to record tremor include accelerometry, electromyography, computer tracking tasks, graphic digitizing tablets and infrared sensor systems (Su *et al*., 2003). Methods to assess tremor can be subdivided into objective quantification techniques and subjective assessments. Subjective assessments are the most common in clinical practice. An objective quantification can be accomplished by employing existing signal processing techniques to the tremor time series. The objective of this study is to design a system that can detect and quantify hand tremor with the intention of opening up a new biomedical application horizon for the state-of-the art haptics research. A major drawback of most of the tremor

**Author for Correspondence: sajith@ee.iitb.ac.in*

recording systems is that the motion sensors have to be worn by the subject and thus it affects the dexterity of the subject. Further the cost of tremor recording system is very high and thus may not be affordable by common man. The present system developed for hand tremor quantification does not affect the dexterity of the subject and is affordable (less than $200) to a common man even for home usage.

Traditional methods of tremor diagnosis use accelerometers (motion sensors) that are placed at different parts of the subject's body. As the subject performs a set of daily activities, these sensors gather the acceleration and orientation information. This is later processed off-line to detect the presence of tremors. Accelerometers may be fixed on the subject's palm and the signals are transmitted to a micro controller for further processing (Harish *et al*., 2009). Measurements have been taken at a sampling rate of 125/250 Hz from subjects with and without tremor. The tremor detection algorithm ran on every 3 sec window of data, and the frequency and amplitude of tremor along all three axes were determined. These two parameters were found to be distinctly different for the tremor and non-tremor cases. Here authors have used a time domain analysis to quantify the tremor frequency and amplitude.

In (Salarian *et al*., 2007), miniature gyroscopes attached to subject's forearms have been used to measure the orientation of movement. Two different methods of measurement were performed: in one, the subjects followed a fixed test protocol and in another the subjects were free to do their day-to-day activities while the measurements were being taken. The latter involved a long measurement time of about 4 hours and therefore a separate system called Autonomous Sensing Unit Recorder (ASUR) was used. Each ASUR unit is a small, independent unit consisting of two gyroscopes, a data-logger, a battery and a flash memory. The angular velocity was obtained by filtering the acquired signal using a band-pass FIR filter with cut-off frequencies of 3.5 Hz and 7.5 Hz. The frequency spectrum of each 3 second window signal was estimated using a 6^{th} order autoregressive model. If the dominant frequency fell between 3.5-7.5 Hz and if its amplitude was sufficiently high, then a tremor was reported in that particular window.

In (Su *et al*., 2003), three dimensional electro-magnetic sensors integrated into a data glove have been used to capture the motion of the hand. Tremor signals were captured during different states like: during rest (to estimate rest tremor), while rotating wrist, grabbing one's hand, etc. Discrete Fourier transform was used to obtain the frequency of the tremor and the instantaneous speed was obtained by computing the derivative of the time domain signal. Further, a 3D electromagnetic imaging system was used to record various features of Parkinson's disease like tremor, rigidity and bradykinesia (Markez *et al*., 2000) developed a tremor quantification device where an electromagnetic tracker was affixed to the finger and data was acquired through a host computer. Frequency and amplitude of tremor were determined. In all of the above methods, the acquired data is analyzed in the frequency domain to obtain the frequency of tremor, since tremor is a pseudo-rhythmic activity and typically there is a frequency associated with each kind of tremor (Harish *et al*., 2009), (Albers *et al*., 1973). The normal hand tremor has a frequency of 9-25 Hz and is of small amplitude. The resting tremor in Parkinson's disease usually ranges from 3-8 Hz (Harish *et al*., 2009).

The use of haptic technology to detect tremors of upper limb has been initially explored in (Bardorfer *et al*., 2001). A virtual environment was created which consisted of a 3D labyrinth like structure. The task given to the subject was to move a ball through the labyrinth from a start to an end point. Various features like the trajectory of the path, collision impact duration and collision impact force were analyzed to identify neurological disorders. Since the task was performed in a virtual environment, it offered the inherent advantage of repeatability of the experiment. Also, labyrinths of various complexities were designed to quantitatively assess the severity of the disease. The results were objective, thus reducing human-factor errors. Even though the advantages are many, this method is not suitable for an accurate spectral analysis of the tremor signal, as the experiment does not provide an adequate time window to observe tremor. There is a chance that even a normal subject may make collision with the walls of the labyrinth and the tremor detection strategy based on the number of collisions is not adequate. The haptic interaction here being more like a pin-ball game, the contacts are impulsive in nature. Thus it does not allow one to collect the continuous tremor data as one would like to. Hence we propose an interaction with a soft object for continuous and prolonged data capturing. Further we prove the utility of the method by cross validating the performance from accelerometer data.

The spectral resolution of fast Fourier transform (FFT) based spectral estimation depends on the duration of the sequence and windowing the sequence implies a reduction in resolution and a leakage over the frequency axis. These factors cause a limitation of the performance of FFT based spectral estimation while dealing with short data segments. The superiority of AR spectral estimate in frequency resolution over FFT based method has been reported based in (Kay and Marple, 1981). This is more so when one is required to identify a few sinusoids in the data, as in the case of tremor signal. Thus we use spectral estimation based on an AR model to estimate the tremor frequency. We also use Choi-Williams distribution (Choi and Williams, 1989) to study if there is any temporal variation in the tremor frequency.

The organization of the paper is as follows. In the next section we provide the design details of haptic rendering of a deformable object. In section III, we provide the details of the experimental set up in which the tremor affected subjects are invited to participate. Section IV presents the pre processing of the haptic and motion sensor data and explains how the motion sensor data is calibrated for comparison with the haptic data. The signal processing requirements have been provided in section V. Experimental results have been presented in section VII, and in the following section the paper concludes.

Virtual Environment Design

In this study, we have explored the use of a virtual environment consisting of a soft object to detect and quantify hand tremors. Rigid objects can be moved by a simple push while moving a soft object is more complex because its shape changes with every interaction and moving it from one location to another usually involves many sequential steps. Some of these steps may involve specific maneuvering to complete the task, prolonging the interaction period which provides a reasonably good time window to observe the tremor, if any. Therefore, we chose a soft object for our 3D environment. Additionally, a soft object is less bouncing for user manipulation and hence it produces a temporally smoother signal (velocity as a function of time) and hence the over-riding tremor signal should be easier to detect from the haptic interaction data. However, rendering of a soft object which is also movable globally is quite difficult. It may be noted that we are implicitly assuming that the user performs a task the same way in the virtual reality environment as one would do in real life. As a protocol we use the elbow as the pivot while interacting with the virtual world. This means that the tremor is limited to the upper part of the hand and eliminates the possibility of any shaking at the shoulder level.

In this work, the subject performs a simple task of moving a virtual soft (deformable) object along a specific direction. Since accelerometer based techniques are quite a proven technology, albeit being of much inferior accuracy, we record velocity of the subjectôs hand movement by both haptic device and accelerometer. These two sets of data are analyzed and compared to see how effective the haptic technique could be in comparison with the common methods using accelerometers. The definite advantage of using haptic technology for tremor diagnosis is that the virtual 3D environment can be altered as and when required to suit the demand of the patient and specific tasks can be designed at various difficulty levels. Haptic environment can provide a full 3D immersion into the virtual world and the accuracy of the task performed is generally high due to unencumbered operation. The position sensor (usually optical) on haptic devices being much more accurate than the accelerometers, we expect a much better accuracy in computing the tremor frequency, if any. Also, since the experiments are conducted under the same protocol for all subjects, this gives rise to a standard method for diagnosis and quantification of tremor. Additionally, with the advent of various gaming platforms, some of the haptic interface devices are available at a very affordable price (about $200), when a patient can have such a measuring device at his/her own home and perform self tests as and when required without the help of any therapist.

The deformation techniques used to model soft objects are either geometry based or physics based. In geometry based techniques, an object is deformed based on structural manipulations. The user manipulates vertices or control points which in turn displaces other vertices for smoother deformations (Coquillart, 1990), (Sederberg and Parry, 1986). However, such deformations are mostly local and are not physically valid. They are also not suitable for global deformation. Physics based deformation techniques model the dynamics involved in interacting with an object and take into account the effects of all the internal and external forces on the shape of the object (Witkin, 1997). But these methods are computationally expensive. However, they do provide an option for simultaneous global deformation and translation of the object. Hence, we use a mass-spring based model of the object, moving under the influence of various internal and external (user applied) forces.

The virtual environment used in our experiments consists of a deformable, thin cylindrical object as shown in Fig. 1.

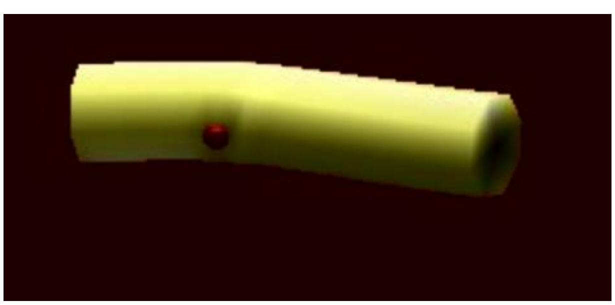

Fig. 1: 3D virtual environment consisting of a thin and soft object being deformed by the haptic device

This may be construed as a small segment of a spaghetti noodle. The geometry of this object was designed such that there are enough number of surface nodes for a good local deformation (Garg, 2011). At the same time, the total number of nodes had to be less to reduce the overall computation time, so that good global deformations and translations are also possible. These factors resulted in the selection of the geometry as shown in Fig. 2.

The object geometry is a damped mass spring model made up of many nodes. The cross- sectional view, as seen in Fig. 2(a), shows a single ring consisting of 8 surface nodes and one internal node. Fig. 2(a) shows a cross section of the trans-axial view of the arrangement of springs. Here O represents the location of the central axis along which (perpendicular to the plane defined by the triangular region AOB) the nodes shown in the cross-section repeat, yielding a long cylindrical structure. The relationship with the nodes along the perpendicular direction is shown in Fig. 2(b) for only the region AOB. Hence Fig. 2(b) shows a sectoral view depicting the positions of the neighbouring nodes. All these nodes have a mass associated with them and are interconnected by springs and dampers. The dampers are very essential to reduce possible oscillations at the constituent springs. Each surface node is connected to 8 other surface nodes and 3 inside nodes. Each central node is connected to 24 surface nodes and 2 neighbouring central nodes. The surface nodes are responsible for local deformation and the central nodes bring about global deformation and translation of the object. The correct estimation of spring stiffness coefficient is vital for the stability and behaviour of the mass-spring model. For the estimation of spring stiffness coefficient, many algorithms have been proposed (Deussen *et. al*., 1995; Lloyd *et al*., 2007). Some of them update the spring stiffness coefficient at each time step and some update the stiffness constant after a few time steps using iterative algorithms. These methods are useful in graphic display where the computations can be relatively slower (at a rate of 30 frames per second) compared to that in haptics here the update has to be at the minimum rate of 1 kHz for the reason of stability. Therefore, the formula proposed in (Gelde, 1998) was

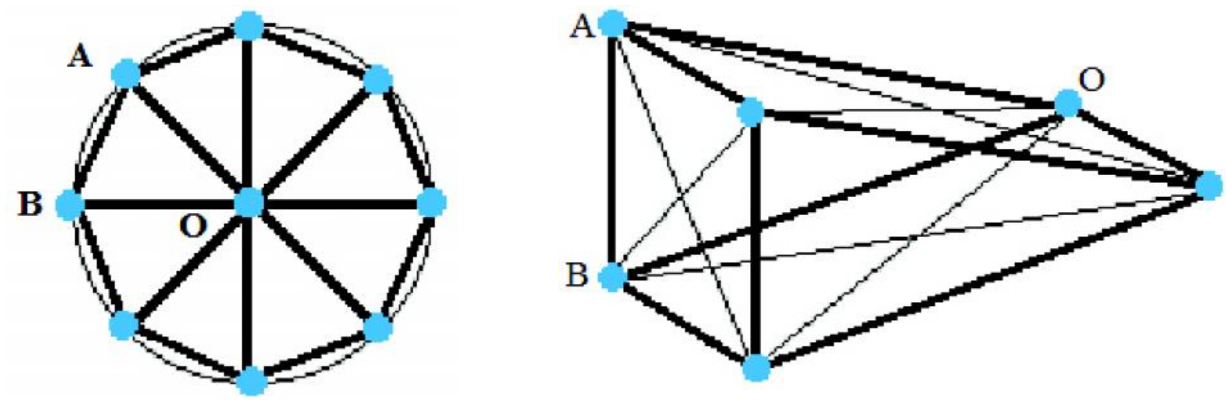

Fig. 2: (a) Cross-sectional view of the cylindrical object with dots indicating the nodes and the straight lines indicating the springs connecting them, (b) a finite volume tetrahedral element, for the wedge shape element ABO showing the diagonal springs [Adapted from: [Anish, 2011]]

used. It is given by

$$k_c = E \sum_e \frac{Vol(T_e)}{|l_c|^2}, \tag{1}$$

Where k_c represents the stiffness coefficient of spring c, l_c is the length of spring c and E is the Youngôs modulus of the material. The summation is over all the tetrahedral elements T_e adjoining c. $Vol(T_e)$ denotes the volume of the tetrahedral element T_e shown in Fig. 2(b). The advantage of using this formula is that the spring stiffness coefficients are pre-computed and valuable computation time is not wasted over their calculations at each time step. Selection of spring damping coefficients are equally important as they prevent the particles of the object from oscillations as mentioned in (Burgin *et al*., 1998). The value of spring damping coefficient k_c^d is taken proportional to the spring constant (Llyod *et al*., 2008) as given by,

$$k_c^d = \alpha k_c. \tag{2}$$

Where α is a positive constant and $0 < \alpha < 1$.

During haptic interaction, collision detection and force computation are the two important problems in rendering. We follow the technique proposed in (Garg, 2011) for the above purposes. The surface node that is closest to the haptic interface point is taken as the collision point. All node positions are updated at every time step. The amount of deformation is dependent on the externally applied force and spring and damper coefficients. The model also takes into account the frictional force between the object and the plane by appropriately selecting the dynamic friction coefficient for the surface. The haptic work space consists of a 10 cm side cube and the subject can interact with the virtual object with a force in the range [0, 5] N.

Experimental Setup

Fig. 3 shows the proposed experimental setup for tremor detection using a haptic environment.

We also show the use of accelerometers in the same setup for cross-validation purposes. Attached to the subjectôs hand is a motion tracker which

Fig. 3: Experimental set-up consisting of both haptic interface and motion sensors

internally contains an accelerometer and a gyroscope. The subject performs a task of moving the virtual object (described in the previous section), placed on a horizontal surface with a haptic device along a specific direction. In the current experiment, the task is to rotate the object by 90^0 about the vertical axis with one of the edges as the centre of rotation. Fig. 4(a) and Fig. 4(b) show the initial and some intermediate positions of the soft object during interaction. The subject moves this object so that it is finally parallel to the reference line as shown in Fig. 4(c). This process takes about 15-20 seconds for a normal subject and may require a longer duration for a subject suffering from hand tremor. The same environment was also visually rendered in 3D using the simple method of anaglyphic stereo. This involves visually rendering the environment as seen from two different camera locations, in two distinct colors, superposed on the same screen. In built functions of OpenGL have been used to implement this.

Anaglyphic glasses are used to view the 3D environment, while performing the haptic task. The haptics API (HAPI) enables us to get the velocity information with which the haptic device is moved. Simultaneously, acceleration and orientation data are also obtained from the motion tracker. Thus, we now have information about subjectôs hand movements through two independent sources (haptic device and motion tracker). However, the start and the end measurement times of the two sources differ because they are started and stopped independently. In order to identify the common data region, as a protocol, the subject shakes his/her hand a little vigorously before starting and after completing the given task, to help synchronize haptic and motion tracker data accurately. This deliberate shake must not be repetitive. Before this entire experiment begins, the subjects are first allowed to get familiarized with the whole system and perform around 10 trials. Then, based on whether they prefer 2D or 3D visual environment, an appropriate display is set-up and the experiments are performed. The 3D visual environment provides a much better hapto-visual immersion of the subject in the virtual world. But the use of anaglyphic lenses may be quite tiresome to the subjectôs vision. It should be noted that the presence of motion sensor on the hand might affect the dexterity of the subject. But, motion sensors are used here just for comparison purposes and to establish in this paper that haptic environment is indeed a good candidate for measuring hand tremor. After establishing the equivalence between the tremor data collected by the haptic device and motion sensors, the rest of the tremor data analysis can be carried out using the data from haptic device alone. It may also be mentioned that any haptic interface device usually has its own inertia (Salisbury *et al*., 1995) and such an inertia may affect the spectral response of the collected signal. We assume the band-width of the haptic device to be much higher than that of the tremor frequency (usually under 10 Hz) so that the effect of mechanical inertia may be neglected.

Pre-Processing

We aim to compare the performances of the

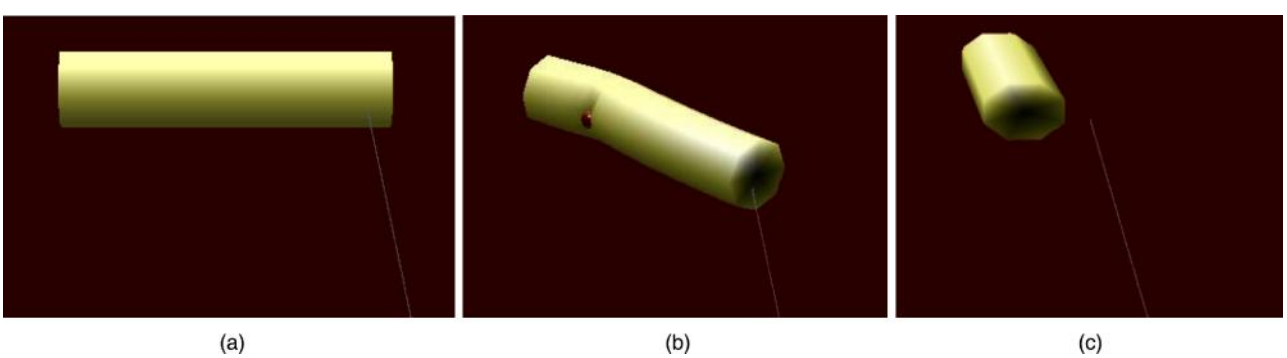

Fig. 4: (a) Initial, (b) some intermediate and (c) final positions of the soft object before, during and after performing the task. The thin line is a reference that helps the subject to align the object to the desired orientation

accelerometer based method with the haptic based method. But the sampling rates and work space axes of the two devices are different. Also, data capturing is asynchronous because the two devices are turned on independently. Further, the sampling rates for the haptic device and the motion sensors are different. Due to these reasons, the following pre-processing steps are required.

(a) Calibration

The data obtained from motion sensors is in the local sensor co-ordinate system. Whenever the subject changes its hand orientation (which definitely occurs while performing the task), the direction of the local co-ordinate system also changes. Thus all the data captured during the task corresponds to values along many different unknown directions. We need to convert all of them to a common co-ordinate system. With the help of the orientation information, this data is converted to the global co-ordinate system using the Following transformation.

$$X_{GS} = R_o^T X_s \tag{3}$$

Where X_s denotes the data from motion sensors in the local sensor co-ordinate system, R_o represents the orientation data available from motion sensors and X_{GS} represents the data in the global co-ordinates system. Since the motion sensor is firmly placed on the palm (outside) used to move the stylus on the haptic device, the translation component can be assumed to be zero. The directions of global co-ordinate system follow a right handed co-ordinate system and are as follows: X-North; Y-West; Z-Vertically up. The orientation calibrated motion sensor data is used for all subsequent processing. It may be noted that the 3D accelerometers measure all accelerations, including the acceleration due to gravity. This is inherent to all accelerometers. Therefore, we remove this component of acceleration due to gravity by subtracting the local mean from the Z-component of the accelerometer data (Pawar *et al*., 2008). Next, the haptic workspace may not coincide with this co-ordinate system. For this, we adjust the haptic device so that the haptic workspace coincides with the global co-ordinate system using a compass. The z-coordinate of the haptic space is aligned to the magnetic north of the compass with x-y plane aligned to the top surface of the table housing the haptic device. Having done that, the position of the haptic device on the table is kept unchanged during subsequent experiments.

(b) Temporal Synchronization

The useful data lies between the deliberate shakes done at the beginning and at the end of the task. These shakes correspond to peaks in the recorded data from both haptic device and accelerometer as shown in Fig. 5 and 6. These peaks are easily identified in both accelerometer and haptic data in all the three axes and the start and the end points from both these sources are matched so that an accurate resampling rate for the haptic data can be calculated to perform the next step. This can be mathematically described as:

$$h_e \triangleq \min(t_{lx}^h, t_{ly}^h, t_{lz}^h) \tag{4}$$

$$h_s \triangleq \max(t_{fx}^h, t_{fy}^h, t_{fz}^h) \tag{5}$$

$$m_e \triangleq \min(t_{lx}^a, t_{ly}^a, t_{lz}^a) \tag{6}$$

$$m_s \triangleq \max(t_{fx}^a, t_{fy}^a, t_{fz}^a) \tag{7}$$

Where $t_{fx}{}^a$, $t_{fy}{}^a$, $t_{fz}{}^a$, $t_{fx}{}^h$, $t_{fy}{}^h$ and $t_{fz}{}^h$ denote the time instants of first peak detected in the accelerometer and haptic data along x, y and z axes, respectively, and $t_{lx}{}^a$, $t_{ly}{}^a$, $t_{lz}{}^a$, $t_{lx}{}^h$, $t_{ly}{}^h$ and $t_{lz}{}^h$ denote the time instants of the last peak detected in the accelerometer and haptic data along *x*, *y* and *z* axes, respectively, h_e and h_s stand for end and start sample indices for the haptic signal, and m_e and m_s are the corresponding indices for the motion sensor data. Thus synchronization means setting $h_s = m_s$ and $h_e = m_e$. To identify the peaks accurately, a bilateral filter (Tomasi and Manduchi, 1998) is applied to both data. This will smoothen the signal without disturbing the peaks corresponding to the initial and final shakes. The peaks are then detected from this smoothed data. For all further processing, the data in-between these peaks are considered. It may be mentioned here that matching the start and the end points by cross correlation cannot be applied as the haptic and motion sensor data are sampled at different rates.

(c) Resampling

In our trials, the haptic sampling rate is about 140 Hz, while the motion tracker used here samples data at the rate of 100 Hz. Therefore, the haptic data is downsampled to match the sampling rate of the motion tracker. The exact downsampling factor D for the haptic signal is given by

$$D = \frac{h_e - h_s}{m_e - m_s}, \tag{8}$$

The 'resample' function of MATLAB is used to down sample the data. Now, both the motion sensor and haptic data are temporally registered, geometrically aligned and correspond to the same sampling frequency of about 100 Hz.

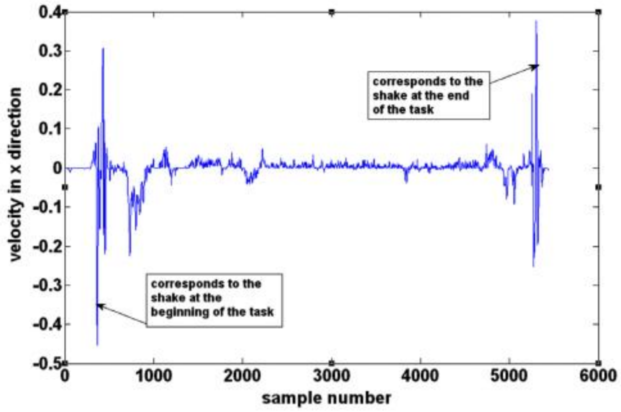

Fig. 5: Velocity signal in x-direction vs sample number as sensed by the hapticdevice

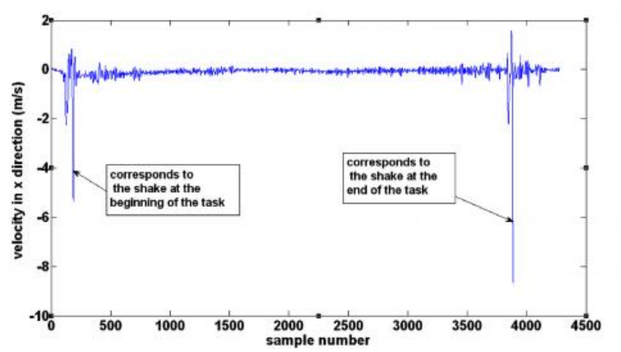

Fig. 6: Velocity signal along x-direction as sensed by the accelerometer

Tremor Data Extraction

The haptic device gives the velocity of hand motion and motion sensor provides the acceleration. Thus the acceleration data from the motion sensor has to be integrated to obtain the velocity. The resultant signal obtained by performing all the steps mentioned above can be considered to be represented as the sum of two components as

$$r(n) = e(n) + f_{tr}(n) \tag{9}$$

with, $r(n)$ denoting baseline data signifying task related hand motion along a particular coordinate axis and $f_{tr}(n)$ denoting the corresponding high frequency tremor component. The base line data (task related hand motion) of the velocity of hand motion along x, y and z directions from the haptic device and motion sensor are computed using an averaging window filter. The estimated base line data at instant n is given by

$$\hat{e}(n) = \frac{\sum_{k=-w_d}^{w_d} r(n+k)}{2w_d + 1} \tag{10}$$

where, w_d denotes the half width of the averaging window.

The averaging filter smoothes the captured velocity of hand motion by removing the higher frequency components and allowing only low

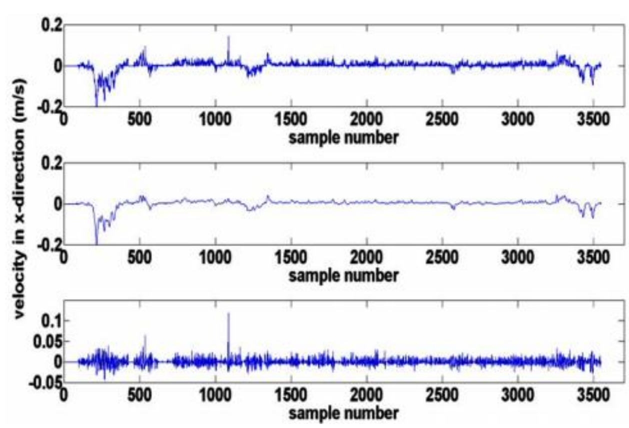

Fig. 7: Plots of haptic data after down sampling (top) the estimated motion trajectory (middle), and the identified hand tremor signal (bottom)

frequency components to pass through. This method also allows us to remove the gravity component along the z-component. Fig. 7 shows an example of the downsampled haptic velocity data and the extracted base line data (motion trajectory). This motion trajectory is then subtracted from the original data $r(n)$ to get only the high frequency components $\hat{f}_{tr}(n)$ as

$$\hat{f}_{tr}(n) = r(n) - \hat{e}(n) \qquad (11)$$

Now $\hat{f}_{tr}(n)$ serves as the estimate of the tremor data. A typical signature of such a hand tremor is also shown in Fig. 7. This data is amenable to different types of signal analysis techniques as described in the next section. Just to illustrate one signal analysis technique, we have considered the power spectral density (PSD), computed using the the periodogram, of the high frequency component $f_{tr}(n)$ to detect the presence of tremors. The PSDs of non-tremor and tremor data from both the haptic device and the motion sensor are shown in Figs. 8 and 9, respectively.

For Fig. 8, we observe that the spectra are quite flat in both cases, signifying that there is no pseudo rhythmic pattern in the data. On the other hand, the PSDs in both cases of Fig. 9 show a distinct peak and the locations are quite close in frequency. This corroborates the fact that the proposed haptics based system is indeed a viable option.

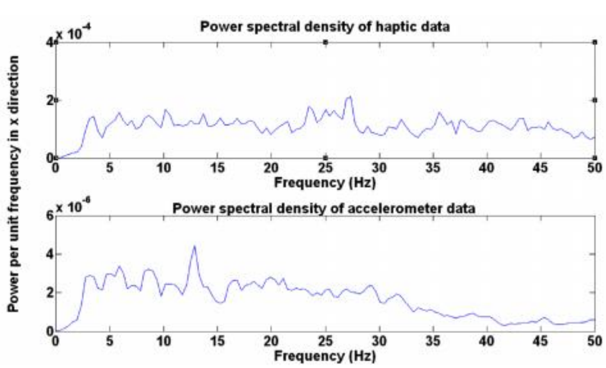

Fig. 8: Power spectral density of non-tremor data for a subject without any visible hand tremor collected from haptic device (top) and accelerometer (bottom) for the component along x-axis

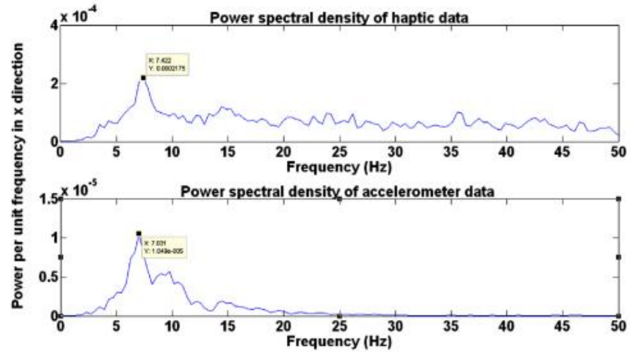

Fig. 9: Power spectral density of tremor data for a subject with visible hand tremor collected from haptic device (top) and accelerometer (bottom) for the component along x-axis

Signal Analysis

We use two different techniques for signal analysis. Since the equivalence between the haptic and the motion sensor data has already been established, we do not show any more results of analysis of the motion sensor data. For the analysis of haptic data, we first use the auto regressive (AR) model fitting to the time series to perform spectral estimation. This provides a good localization of the tremor frequency. Subsequently we perform a time frequency analysis of the data using the Choi-Williams method. The purpose of the study is to observe if there is a temporal variation in the tremor frequency.

(a) AR Modelling

A spectrum that is characterized by its peaks, as opposed to valleys, can be modeled well by an AR model, thus making AR modeling the most appropriate method for the analysis of tremor data. Two steps are involved in the modelling of tremor data using an AR model. First is the selection of a proper model order (p) and second is the estimation of model parameters from the data. Here the data is modelled by the following difference equation

$$f_{tr}(n) = \sum_{k=1}^{p} a_k \, f_{tr}(n-k) + w(n) \qquad (12)$$

where, $w(n)$ is a white noise, a_k are the AR parameters and $f_{tr}(n)$ is the tremor data. The power spectral density of the tremor data is given by

$$P_{ftr}(f) = \sigma_w^2 |H(f)|^2 \quad (13)$$

where, $P_{ftr}(f)$ is the power spectral density of the tremor data, $\sigma_w{}^2$ is the noise power and $H(f)$ is the frequency response of the model. The AR parameter estimation is done by using Burgs algorithm (Burg, 1968). The AR model order p is estimated by using the Akaike information criterion (AIC) (Akaike, 1974) and is based on selecting the order that minimizes

$$AIC(p) = \ln \hat{\sigma}_{wp}^2 + \frac{2p}{N} \quad (14)$$

Where, $\hat{\sigma}_{wp}^2$ is the estimated noise variance and N is the length of the data sequence. In the present work we identified that a 6th order AR model can fit the tremor data received from different subjects very well.

(b) Choi-Williams Spectrum

Time frequency signal representations characterize signals over a time frequency plane (Cohen, 1989). These kinds of analysis tools give a temporal localization of a signal's spectral components. Time frequency representations map an input signal $f_{tr}(n)$ into a two dimensional function of time and frequency, $T_{ftr}(n, f)$. This technique has been used to analyze non-stationary or time varying signals. Wigner-Ville distribution (WVD) is a member of Cohen class time-frequency distributions (Cohen, 1989). The well known Cohen class distribution is given by

$$C_{ftr}(i,k) = \sum_{m=-L/2}^{+L/2} \sum_{n} \phi(n,m) R(i-n,m) e^{-j2\pi km/L} \quad (15)$$

where $R(i, m)$ is the auto correlation function of the tremor signal and $\phi(n, m)$ is the kernel function. Here L is the window length and the variable n is also varied across an appropriate window. Compared to short-time Fourier transform based method of time frequency analysis, this method can yield a better time frequency resolution. The Wigner-Ville distribution of a signal is obtained by correlating the signal with a time shifted version of the signal itself and the WVD of a signal $f_{tr}(n)$ is defined as

$$DWVD_{ftr}(n, f) = 2 \sum_{m=-\infty}^{+\infty} f_{tr}\left(n + \frac{m}{2}\right) f_{tr}^*\left(n - \frac{m}{2}\right) e^{-j2\pi fm} \quad (16)$$

WVD can be computed efficiently using a fast Fourier transform (FFT) (Swami and Mendel). One major drawback of WVD is the presence of cross term or interference term as WVD is quadratic in nature. The amount and the shape of this interference are directly related to the Particular kernel function $\phi(n, m)$ which is unity for WVD. Choi and Williams (Choi and Williams, 1989) proposed the use of an exponential kernel

$$\phi(n,m) = \exp\left(\frac{-n^2 m^2}{\sigma^2}\right) \quad (17)$$

to reduce the cross terms, but at the same time preserving most of the properties of WVD. The parameter σ controls the attenuation of the cross terms. However, increasing σ leads to a loss of spectral resolution. As a compromise we choose a value of σ equal to 0.5.

Experimental Results

The virtual environment was created using Visual Studio 2005 and the HAPI libraries. HAPI is a open source high level haptic API developed by Sense Graphics. HAPI is written in the C++ programming language and works on all major operating systems. HAPI provides a number of haptic force effects, surface effects, collision detection, primitive shape creation and thread handling in addition to the basic device handling. We use Novint FALCON, a commercially available haptic gaming platform in the prize range of $200, as the haptic device to interact with the virtual world. For motion data, we use Xsens sensors. Data from the motion tracker was transmitted to a computer via an USB cable. The captured data was processed offline in MATLAB on a Intel Core-2-Quad processor system with 8 GB RAM and a processing speed of 2.6 GHz working under Windows XP Operating system.

A normal subject is first asked to interact with the virtual soft object through the FALCON and the experience of the user is noted down. As the number of nodes in the object is increased, the haptic experience improves, signifying a smoother interaction. However, this increases the computation time for haptic rendering and one may not be able to complete the rendering within 1ms. Therefore, a GPU based rendering would be more useful to the user. Since all our computations are performed in the CPU, we had to restrict the number of nodes to 180. If the gap increases between two successive nodes along the length of the object, there could be a possibility of piercing through the object during interaction if a large amount of force is applied. This is a short-coming of the developed system which hopefully can be solved by introducing more number of nodes to model the object and by implementing it on a GPU. In order to have a better hapto-visual immersion into the 3D environment, the visual rendering was performed on a stereoscopic display by superimposing the images for two different viewpoints. An anaglyphic lens is used by the subject to perceive the depth during haptic interaction. A number of tremor affected volunteers are asked to interact with the created virtual environment and the velocity of hand motion is captured using the haptic device. The captured velocity data is subjected to tremor extraction routine discussed in section V. The power spectrum estimated using the AR model of two representative subjects are shown in Fig. 10 and Fig. 11.

The frequency corresponding to the peak value is 4.6 Hz in subject 1 and 7.0 Hz in subject 2. These frequencies are in accordance with (Harish *et al*., 2009). From both the plots, one can see a distinct peak in the spectrum. This indicates that the subject indeed has hand tremor, which is verified from the known history of the subject. These results illustrate the usefulness of the proposed method.

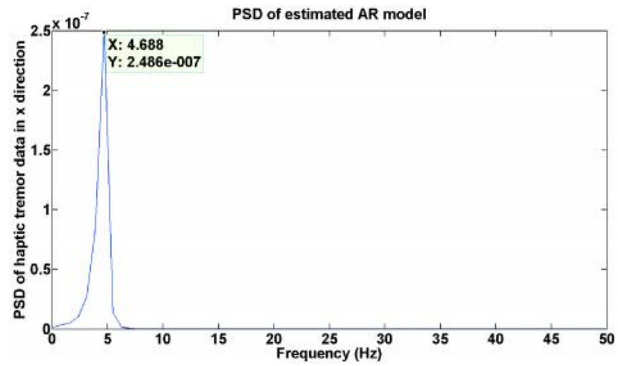

Fig. 10: PSD of haptic tremor data from subject 1 along x-direction

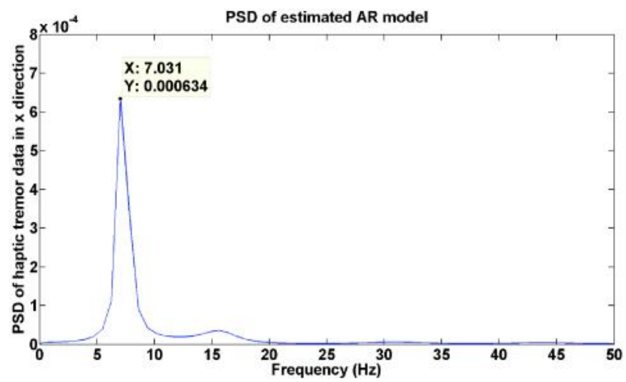

Fig. 11: PSD of haptic tremor data from subject 2 along x-direction

The Choi-Williams spectrum is used to see if there is any temporal variation in tremor frequency. The Choi-Williams spectra from two representative subjects are plotted in Figs. 12 and 13.

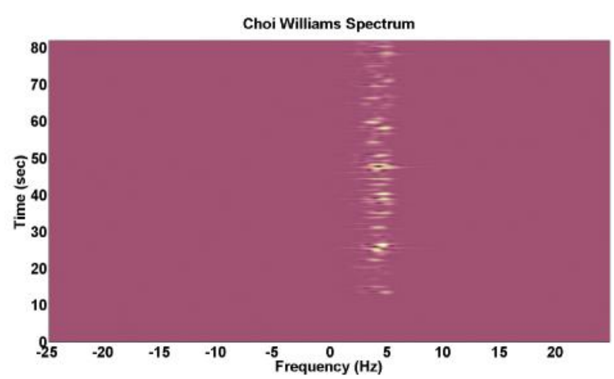

Fig. 12: Choi-Williams spectrum of tremor data for subject 1 along x-direction

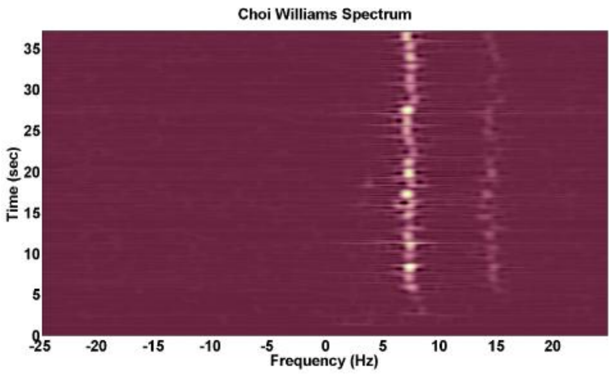

Fig. 13: **Choi-Williams spectrum of tremor data for subject 2 along x-direction**

From these two plots, we do not observe any noticeable change in the spectral content temporally. This suggests that both subjects had a fairly constant tremor frequency and it did not change during different phases of performing the haptic task. This further demonstrates that the proposed technique is quite reliable as there is no drift in frequency while performing the haptic task. In all these illustrations, we have given the spectral plots of tremor data along x-axis. Since the motion of the object is restricted to x-y plane only (as the object rests on the horizontal plane $z = 0$), we have also analyzed the tremor along the y-axis, and the corresponding results are found to be very similar. Hence they are not reproduced here.

Conclusions

We have proposed the use of a deformable object manipulation in a virtual 3D haptic environment as a method of tremor data acquisition. We collected data from several subjects, in the age group of 60-65, having tremor.We have been able to identify the presence of tremors based on the power spectral density of tremor signal in the velocity data, obtained from the haptic device. We have compared the proposed haptic based method with the most commonly used accelerometer based method and found the consistency of results from both the methods, thus experimentally validating our idea. Further, we are able to fit an AR model to the tremor data and estimate the PSD using the AR model. The haptic based method does not require any re-calibration as required by accelerometer based method. Further by designing different types of deformable objects and interaction plan, any kind of tremor could be measured and quantified. In this paper our emphasis has been purely on developing a general purpose haptic system for measurement of hand tremor. The task of identifying various types of hand tremors and the progression analysis of tremor condition after appropriate rehabilitation remains to be investigated. Further the effect of loading during the task performance needs to be studied for an appropriate subject base.

Acknowledgment

We sincerely thank all the subjects who volunteered to participate in our experiments. Partial funding from both DST Govt. of India, New Delhi and DEITY, Govt. of India, New Delhi, is gratefully acknowledged.

References

Akaike H (1974) A new look at the statistical model identification, *IEEE Transactions on Automatic Control* AC-19, 716-723

Albers J W, Potvin A R, Tourtellotte W W, Pew R W and Stribley R F (1973) Quantification of Hand Tremor in the Clinical Neurological Examination, *IEEE Transactions on Biomedical Engineering* BME-20, 27-37

Bardorfer A, Munih M, Zupan A and Primozic A (2001) Upper limb motion analysis using haptic interface, *IEEE/ASME Transactions on Mechatronics* **6** 253-260

Burg J P (1968) A new analysis technique for time series data, NATO advanced study institute on signal processing with emphasis on underwater acoustics **83** 12-23

Burgin J, Stephens B, Vahora F, Temkin B, Marcy W, Gorman P J and Krummel T M (1998) Haptic rendering of volumetric soft- bodies objects, Proceedings of Third PHANTOM Users Group Workshop, Massachusetts Institute of Technology, Cambridge, 9-13

Choi H I and Williams W J (1989) Improved time-frequency representation of multicomponent signals using exponential kernels, *IEEE Transactions on Acoustics*, *Speech and Signal Processing* **37** 862-871

Cohen L (1989) Time-frequency distributions-a review, *Proceedings of the IEEE* **77** 941-981

Coquillart S (1990) Extended Free-Form Deformation: A sculpturing Tool for 3D Geometric Modeling, *Proceedings of SIGGRAPH Computer Graphics* **24** 187-196

Deussen O, Kobbelt L and Tucke P (1995) Using simulated annealing to obtain good nodal approximations of deformable bodies *Proceedings of Eurographics Workshop on Computer Animation and Simulation* 30-43

Garg A (2011) Haptic Rendering of 3D objects - M.Tech Thesis, Indian Institute of Technology Bombay

Gelde A V (1998) Approximate simulation of elastic membranes by triangulated spring meshes *Journal of Graphics Tools* **3** 21-42

Harish K, Rao M V, Borgohain R, Sairam A and Abhilash P (2009) Tremor quantification and its measurements on Parkinsonian patients, International Conference on Biomedical and Pharmaceutical Engineering *ICBPE '09* 1-3

Kay S M and Maple S L (1981) Spectral analysis - a modern perspective *Proceedings of IEEE* **69** 1380-1419

Lloyd B A, Szekely G and Harders M (2007) Identification of Spring Parameters for Deformable Object Simulation, *IEEE Transactions on Visualization and Computer Graphics* **13** 1081-1094

Lloyd B A, Kirac S, Szkely G and Harders M (2008) Identification of dynamic mass spring parameters for deformable body simulation, Eurographics - Short Papers, (Eds: Mania K and Reinhard E) 131-134.

Markez S (2000) Development of a Hand Tremor Quantification Device for the Measurement of Pathological Tremor, A thesis in Master of Health Science, Institute of Biomaterials and Biomedical Engineering, University of Toronto

Pawar T, Anantakrishnan N, Chaudhuri S and Duttagupta S (2008) Impact of Ambulation in Wearable ECG *Annals of Biomedical Engineering* **36** 1547-1557

Rocon E, Belda-Lois J M, Sanchez-Lacuesta J J and Pons J L (2004) Pathological Tremor management: Modelling, compensatory technology and evaluation *Technology and Disability* **16** 3-18

Salarian A, Russmann H, Wider C, Burkhard P R, Vingerhoets F J G and Aminian K (2007) Quantification of Tremor and Bradykinesia in Parkinson's Disease Using a Novel Ambulatory Monitoring System *IEEE Transactions on Biomedical Engineering* **54** 313-322

Salisbury K, Brock D, Massie T, Swarup N and Zilles C (1995) Haptic Rendering: Programming Touch Interactions with Virtual Objects, Proceedings of the ACM Symposium on Interactive 3D Graphics.

Sederberg T W and Parry S R (1986) Free-form deformation of solid geometric models *ACM SIGGRAPH Computer Graphics* **20** 151-160

Swami A, Mendel J M and Nikias C L, Higher order spectral analysis toolbox with Matlab, http://www.mathworks.com/matlabcentral/fileexchange/3013

Su Y, Allen C R, Geng D, Burn D, Brechany U, Bell G D and Rowland R (2003) 3-D motion system (data-gloves): application for Parkinson's disease *IEEE Transactions on Instrumentation and Measurement* **52** 662-674

Tomasi C and Manduchi R (1998) Bilateral Filtering for Gray and Color Images *Proceedings of the IEEE International Conference on Computer Vision* 839-846

Witkin A (1997) An Introduction to Physically Based Modeling: Particle System Dynamics, SIGGRAPH course notes.